

Modularity of the Wrist in Extant Hominids

Ana Bucchi^{1,2}, Thomas A. Püschel³, Antonio Profico⁴, Carlos Lorenzo^{1,2}

¹Universitat Rovira i Virgili, Departament d'Història i Història de l'Art, Avinguda de Catalunya 35, 43002 Tarragona, Spain.

²Institut Català de Paleocologia Humana i Evolució Social (IPHES), Zona Educacional 4, Campus Sescelades URV (Edifici W3), 43007 Tarragona, Spain

³Primate Models for Behavioural Evolution Lab, Institute of Cognitive and Evolutionary Anthropology, School of Anthropology, University of Oxford, 64 Banbury Road, OX2 6PN, Oxford, United Kingdom.

⁴PaleoHub, University of York, Wentworth Way Heslington, YO10 5NG York, United Kingdom

Correspondence: Ana Bucchi, Universitat Rovira i Virgili, Departament d'Història i Història de l'Art, Tarragona, Spain. email: anabucchi@gmail.com

Abstract

Wrist shape varies greatly across primates and previous studies indicate that the numerous morphological differences among them are related to a complex mixture of phylogeny and function. However, little is known about whether the variation in these various anatomical differences is linked and to what extent the wrist bones vary independently. Here, we used 3D geometric morphometrics on a sample of extant hominids (*Homo sapiens*, *Pan troglodytes*, *Gorilla gorilla*, and *Gorilla beringei*), to find the model that best describes the covariation patterns among four of the eight carpals (i.e., capitate, lunate, scaphoid, and trapezium). For this purpose, 15 modular hypotheses were tested using the Covariation Coefficient. Results indicate that there is a covariation structure common to all hominids, which corresponds to stronger covariation within each carpal as compared to the covariation between carpals. However, the results also indicate that there is a degree of codependence in the variation of some carpals, which is unique in humans, chimpanzees, and gorillas, respectively. In humans there is evidence of associated shape changes between the lunate and capitate, and between the scaphoid and trapezium. This covariation between lunate and capitate is also apparent in gorillas, while chimpanzees display the greatest disassociation among carpals, showing low covariation values in all pairwise comparisons. Our analyses indicate that carpals have an important level of variational independence which might suggest a high degree of independent evolvability in the wrists of hominids, and that although weak, the structure of associated changes of these four carpals varies across genera. To our knowledge this is the first report on the patterns of modularity between these four wrist bones in the Homininae and future studies might attempt to investigate whether the anatomical shape associations among carpals are functionally related to locomotion and manipulation.

Key words: modularity; trait covariation; wrist; hominids

Introduction

The wrist in hominids is composed of eight bones with complex shapes and numerous joint surfaces, which allow the hand to move along multiple axes (Kivell et al., 2016). Genetically, a common Hox gene expression regulates the development of the hand in anthropoids (Reno et al., 2008), yet carpals also have a degree of functional and evolutionary independence (Tocheri et al., 2003; Kivell et al., 2013). This functional and evolutionary independence may explain why carpal morphology varies so greatly across taxa (Tocheri et al., 2005; Marzke et al., 2010; Orr, 2017).

Among primates, humans exhibit a derived carpal morphology (Kivell et al., 2016), which previous studies suggest evolved as a consequence of relaxed locomotor pressures with the advent of bipedalism and as an adaptation to tool making and use (Hamrick et al., 1998; Williams et al., 2010; Key and Dunmore, 2015; Skinner et al., 2015; Kivell et al., 2016). Wrist morphology in humans contributes significantly to stone tool-making performance (Tocheri et al., 2003; Marzke et al., 2010; Williams et al., 2010, 2014), and some carpal features in humans that have been thought to be beneficial for this activity include the size, orientation, and degree of curvature of joint surfaces at the trapezium, capitate, and radiocarpal joints (Marzke, 1983, 1997; Niewoehner et al., 1997; Richmond and Strait, 2000; Tocheri et al., 2003, 2005; Marzke et al., 2010; Williams et al., 2010, 2014; Orr, 2017). The characteristic joint surfaces in the human wrist allow for increased accuracy (Williams et al., 2014) and mechanical work at the joint during stone tool production (Williams et al., 2010). They also allow toolmakers to effectively resist and transmit both axial and oblique joint reaction forces generated by power and precision grips as compared to the rest of the extant apes (Marzke, 1983; Niewoehner et al., 1997). Conversely, the wrist in chimpanzees and gorillas seems better adapted to locomotor demands, by contributing to better stabilization at the joint (Tuttle, 1967; Richmond and Strait, 2000) and by allowing the joint to better withstand the stresses imposed by knuckle walking (Püschel et al., 2020).

Several previous studies have analyzed single bones and specific joint surfaces with the aim of inferring the functional capabilities that set apart hominins from non-human primates (e.g., Tocheri et al., 2003, 2005; Marzke et al., 2010; Kivell, 2011). However, with some exceptions (Williams, 2010; Peña, 2018), there are almost no studies analyzing whether the numerous shape variations in wrist bones are associated or independent with respect to each other. Peña (2018) proposes that the level of integration of the wrist is higher in some primate genera (i.e., *Pongo*) than others, suggesting that specific covariation patterns may be shaping the evolution of this structure in primates. For humans, previous studies indicate that the morphological integration of autopods is lower than in quadrupeds, making the human hand more evolvable (Rolian, 2009; Rolian et al., 2010; Young et al., 2010). However, Williams (2010) indicates that the patterns of integration of the capitate and third metacarpal are more similar between humans and gorillas than between gorillas and chimpanzees, and that knuckle-walkers are not characterized by highly integrated morphologies.

The mutual relationships between bony elements of a single structure are best studied within the framework of modularity as they allow us to know how flexible the evolution of this anatomical region is under differing functional demands. If all carpals behave as a single entity that is tightly integrated by strong interactions, they should comprise a module (Klingenberg, 2008; Esteve-Altava, 2017), thus causing wrist bones to covary strongly. Conversely, if more than one module is present in the wrist, this should cause carpals in different modules to vary independently. It is currently unknown how many modules there are in the primate wrist, and how strong the modular signal is.

Our analysis intends to address the question of how independent the variation within the wrist is by analyzing the modularity pattern of four carpals in extant hominids (i.e., the capitate, trapezium, lunate, and scaphoid). As far as we know, this is the first time that the covariation structure for these bones has been reported for modern humans (*Homo sapiens*), chimpanzees (*Pan troglodytes*), and gorillas (*Gorilla gorilla* and *Gorilla beringei*). 3D models and geometric morphometrics were used for this purpose, and modularity was investigated through the testing procedure proposed by Adams and Collyer (2019), known as the covariance ratio effect sizes (Z_{CR} and $\hat{Z}12$). We tested 15 different modular hypotheses combining all possible partitions of the wrist bones and selected the one that best describes the covariation structure in hominids as a whole, and in humans, chimpanzees, and gorillas in particular. In doing so, we try to answer two main questions: a) what is the modularity pattern of these four bones in living hominids? and b) is the observed covariation pattern shared across the analyzed taxa? We hypothesize that humans exhibit a pattern of covariation that distinguishes them from African apes, based on previous studies suggesting that manipulation has driven the evolution of the wrist in humans (e.g., Williams et al., 2010; Key and Dunmore, 2015; Skinner et al., 2015), while in apes its better adapted for locomotion (e.g., Richmond and Strait, 2000; Püschel et al., 2020).

Materials and methods

Primate sample

The sample comprises 478 bones from three primate genera: 50 modern humans (*Homo sapiens*), 41 chimpanzees (*Pan troglodytes*), and 41 gorillas (19 *Gorilla gorilla* and 22 *Gorilla beringei*) (Table 1). 3D models came from different sources. All human surface models were obtained using a Breuckmann SmartSCAN structured light scanner (Breuckmann Inc.). Most non-human primate surface models were generated via photogrammetry (further details can be found in Bucchi et al., 2020), while CT scans of 23 ape hands were accessed from two different digital repositories: Morphosource (www.morphosource.org) and the Museum of Primatology (<https://carta.anthropogeny.org/>).

The resolutions of micro-CT, surface scanner, and photogrammetric models have been previously tested and found to be comparable (Giacomini et al., 2019) thus allowing us to combine these data types in our analyses. The human hands belonged to a medieval cemetery (Burgos, Spain) (Casillas García and

Adán Álvarez, 2005) and the non-human sample were of different origins (wild shot, in captivity, and of unknown provenance). Right hands were preferred. Most of the wrists included the four carpals under analysis, and when there were some missing bones, their antimeres, when present, were reflected using the ‘Flip and/or Swap axis’ and ‘Invert faces orientation’ tools in Meshlab software (v. 2020.02) (Cignoni et al., 2008).

We analyzed the morphology of four carpals (i.e., the capitate, trapezium, lunate, and scaphoid), although not all individuals had all of these bones (some elements were missing in some cases; further details can be found in Table 1 and in Supp. Table S1).

Table 1 The study sample. UBU: Universidad de Burgos, AM: AfricaMuseum, IPHES: Catalan Institute of Human Palaeoecology and Social Evolution, MZB: Natural Sciences Museum in Barcelona, and ZSM: Zoological State Collection in Munich.

Species	Specimens	Carpal bones				Sex			Collection
		TM	SC	CA	LU	Male	Female	Unknown	
<i>Homo sapiens</i>	50	40	39	41	42	25	25	0	UBU
<i>Pan troglodytes</i>	41	38	41	40	38	16	14	11	AM, ZMB, ZCM, Morphosource, Museum of Primatology
<i>Gorilla beringei</i>	22	22	22	22	21	10	9	3	
<i>Gorilla gorilla</i>	19	17	18	19	18	5	5	9	
Total	110	117	120	122	119	56	53	24	

Landmark configuration

We acquired five fixed landmarks per bone (Fig. 1 and Table 2). Landmark coordinates were imported into R using the *Arothron* package version 1.1.1 (Profico et al., 2018) in R 1.2.5019 (R Core Team, 2019). A generalized Procrustes analysis (GPA) was then performed separately for each bone in order to normalize for location, rotation, and scale. Corrected coordinates were then compiled into a new dataframe, and hypotheses of modularity were tested (see below).

Allometry

Taxonomic differences in size can affect the pattern and magnitude of modularity (Klingenberg and Marugán-Lobón, 2013). Therefore, we tested for allometric signals in the data by using a regression of Procrustes shape variables on centroid size. This test was performed with the *procD.lm()* function of

the *geomorph* package, version 3.2.1 (Adams et al., 2019). Note that in order to have balanced sample sizes, this and all further statistical analyses were carried out by pooling both gorilla species together.

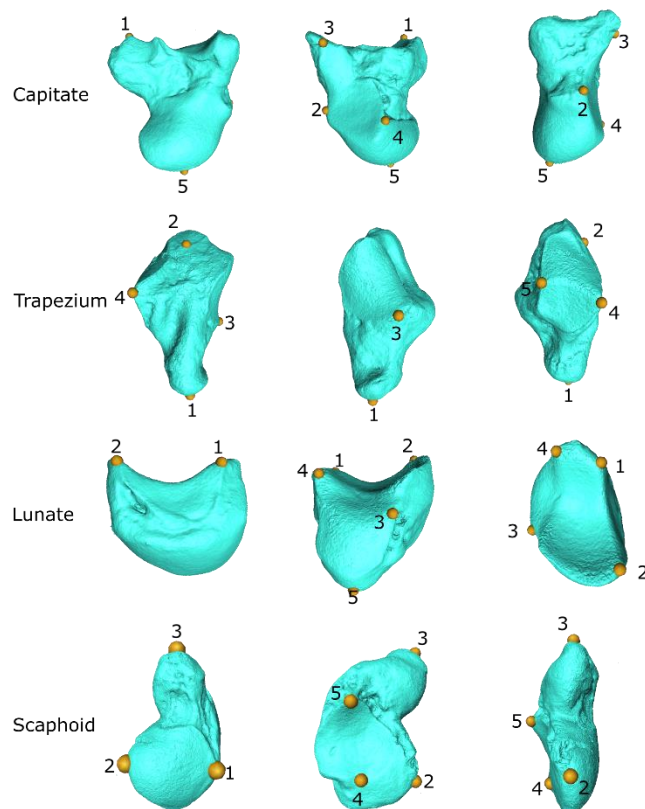


Figure 1 The landmark configuration shown on specimen AM 998 (*Gorilla beringei*) for the capitate, trapezium, lunate, and scaphoid bones. Landmark definitions are provided in Table 2.

Modular hypotheses

We tested 15 different hypotheses of modularity corresponding to all possible partitions of the sample (Table 3). We defined one four-module model (H1), seven two-module models (H2-8), six three-module models (H9-H14), and one single-module model. The optimal modular hypothesis for the wrist was assessed by measuring the strength of covariation for each modular hypothesis with the covariance ratio (CR) (Adams, 2016) and then statistically comparing alternative modular hypotheses with the covariance ratio effect sizes (Z_{CR} and $\hat{\chi}^2_{12}$) (Adams and Collyer, 2019).

Covariance ratio (CR)

The covariance ratio (CR) (Adams, 2016) was computed to measure the degree of modular signal in two or more *a priori* modules of Procrustes shape variables. The CR coefficient calculates the ratio of the overall covariation between modules relative to the overall covariation within modules (Adams,

2016). The CR coefficient ranges from 0 to positive values. CR values lower than 1 indicate low covariation between modules, and strong covariation otherwise. The significance of the CR coefficient is assessed via permutations. At each repetition, landmarks are randomly assigned to different modules and the CR coefficient is calculated. The original CR value is then compared to the CR distribution (Adams, 2016).

Table 2 Definitions of landmarks digitalized in this study.

Bone	Landmark	Position
Capitate	1	Most anterior point of the union between the facets for the second and third metacarpals.
	2	Most distal and posterior point of the union of the facets for the hamate and the lunate.
	3	Most distal point of the facet for the hamate.
	4	Most inferior and anterior point of the union of facets for the hamate and the lunate.
	5	Point of maximum curvature of the lunate-scaphoid facet.
Trapezium	1	Point of maximum curvature of the ridge of the trapezium.
	2	Most anterior point of the facet for the second metacarpal.
	3	Most lateral and proximal point of the facet for the first metacarpal.
	4	Most anterior point of the union between the facets for the trapezoid and the scaphoid.
	5	Most posterior point of the union between the facets for the trapezoid and the scaphoid.
Lunate	1	Most posterior and distal point of the facet for the scaphoid.
	2	Most anterior and distal point of the facet for the scaphoid.
	3	Most anterior point of the intersection between the facets for the triquetral and the hamate.
	4	Most posterior point of the intersection between the facets for the hamate and capitate.
	5	Point of maximum curvature of the facet for the radius.
Scaphoid	1	Most posterior point of the facet for the radius.
	2	Most anterior point for the facet for the radius.
	3	Point of maximum curvature of the tubercle of the scaphoid.
	4	Most medial point of the facet for the capitate.
	5	Most lateral point of the facet for the capitate.

Table 3 The 15 modular hypotheses tested in this study. CA=capitate, LU=lunate, SC=scaphoid, and TZM= trapezium.

Model hypotheses	Modules	Description
H1	CA-LU-SC-TZM	All carpals belong to different modules.
H2	CALU-SCTZM	The capitate and lunate belong to one module and the scaphoid and trapezium to another.
H3	CASC-LUTZM	The capitate and scaphoid belong to one module and the lunate and trapezium to another.
H4	CATZM-LUSC	The capitate and trapezium belong to one module and the lunate and scaphoid to another.
H5	CA-LUSCTZM	The capitate belongs to one module and the lunate, scaphoid, and trapezium to another.
H6	LU-CASCTZM	The lunate belongs to one module and the capitate, scaphoid, and trapezium to another.
H7	SC-CALUTZM	The scaphoid belongs to one module and the capitate, lunate, and trapezium to another.
H8	TZM-CALUSC	The trapezium belongs to one module and the capitate, lunate, and scaphoid to another.
H9	CALU-SC-TZM	There are three modules: one includes the capitate and lunate, the second includes the scaphoid, and the third includes the trapezium.
H10	CASC-LU-TZM	There are three modules: one includes the capitate and scaphoid, the second includes the lunate, and the third includes the trapezium.
H11	CATZM-LU-SC	There are three modules: one includes the capitate and trapezium, the second includes the lunate, and the third includes the scaphoid.
H12	LUSC-CA-TZM	There are three modules: one includes the lunate and scaphoid, the second includes the capitate, and the third includes the trapezium.
H13	LUTZM-CA-SC	There are three modules: one includes the lunate and trapezium, the second includes the capitate, and the third includes the scaphoid.
H14	SCTZM-CA-LU	There are three modules: one includes scaphoid and trapezium, the second includes the capitate, and the third includes the lunate.
H15	CALUSCTZM	All carpals belong to one module

Comparing the strengths of the modular signals (Z_{CR} and \hat{Z}_{12})

The covariance ratios effect size (Z_{CR}) is derived from the CR and is a standardized test statistic which ensures statistical compatibility with the CR (Adams and Collyer, 2019) (Table 1). When the observed CR is larger than expected under the null hypothesis of no modularity, the Z_{CR} exhibits greater negative values which indicates a stronger modular signal. Here, whether Z_{CR} values are statistically different from each other was evaluated using a two sample Z-score for comparing modular signals (\hat{Z}_{12}). Both metrics are needed to compare alternative modular hypotheses. Z_{CR} was calculated for all modular hypotheses and the model presenting the strongest modular signal (i.e., the lowest Z_{CR}) was selected as

the optimal modular hypothesis for all samples, and for each genus separately. Once the best hypothesis was identified, we also tested whether some genera displayed a greater degree of modularity than others. The CR, Z_{CR} , and \hat{Z}_{12} were also calculated using the *modularity.test()* and *compare.CR()* functions of the *geomorph* R package (Adams et al., 2019).

All the data used in this study are available in Supplementary Material 1 (Table S1). These data comprise the landmark coordinates after Procrustes superimposition.

Results

Allometry

Regression analyses of Procrustes coordinates on centroid size produced non-significant results in all cases ($p > 0.05$). Therefore, we excluded size as a factor contributing to variation in shape among the taxa studied here, and the following analyses were carried out using Procrustes coordinates and not ‘size-corrected’ variables (i.e., the residuals from the regressions of shape on centroid size).

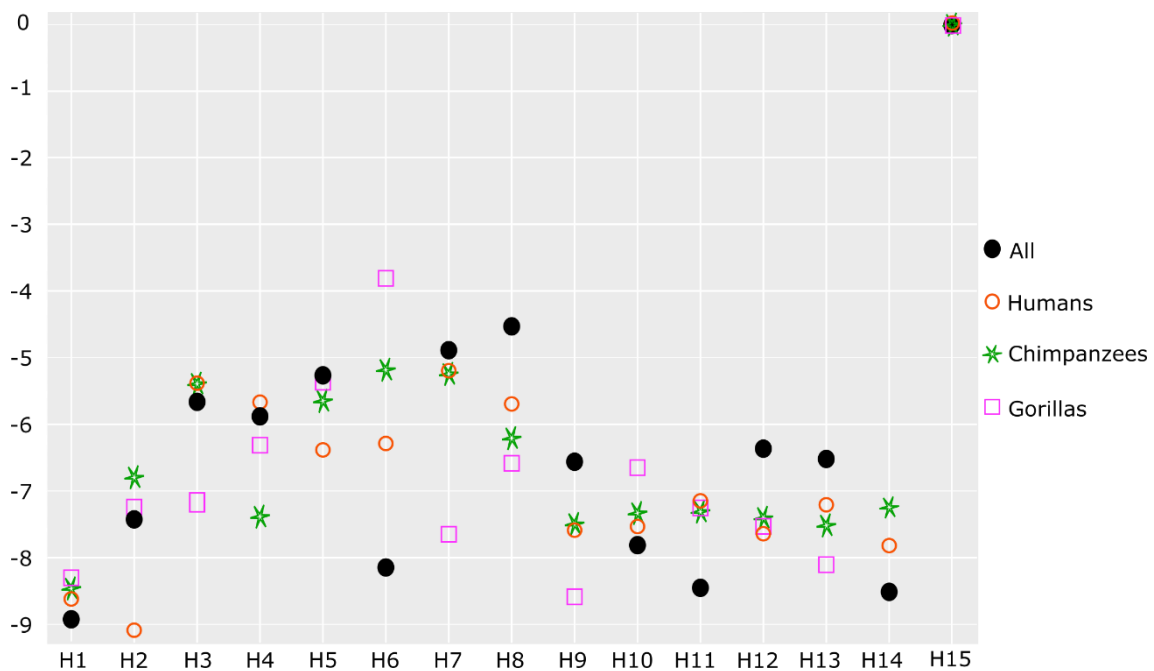


Figure 2 Effect sizes (Z_{CR}) for the covariance ratio (CR) for the 15 modular hypotheses for all samples, and for each genus separately. Hypotheses are described in Table 3. The exact Z_{CR} values are in Table 4 and the pairwise differences in Z_{CR} (\hat{Z}_{12}) are in Tables S3-6.

Optimal modular hypotheses for hominids.

The CRs of all hypotheses were significantly less than 1 (Table 4), indicating that regardless of how the bones are combined to create the alternative modular hypotheses there is a strong modular signal in the sample. When comparing all hypotheses, H1 for the whole sample exhibited the largest negative Z_{CR} (Fig. 2, Table 4) which was significantly different ($p < 0.05$) from all the remaining hypotheses (Fig. 2, Table S6). H1 was thus selected as the best modularity model for hominids, which implies that each carpal represented is its own modular unit. However, except in chimpanzees (Fig. 2 and 3, Table 4), H1 was not the best modular model for each genus individually. In humans, H2 showed a larger negative Z_{CR} than H1 (Fig. 2, Table 4), although this difference was not significant ($\hat{Z}_{12} = 0.63$, $p = 0.53$) (Table S3). Model H2 implies that the capitate and lunate form a different module than that of the scaphoid and trapezium. In gorillas, H9 yielded a larger negative Z_{CR} than H1 (Fig. 2, Table 4), yet this difference was not statistically significant either ($\hat{Z}_{12} = 0.43$, $p = 0.67$) (Table S5). H9 groups the capitate and lunate in the same module, while the scaphoid and trapezium each belong to their own modules. Figure 3 depicts the optimal modular hypothesis for each genus.



Figure 3 Illustration of the dorsal view of a left wrist showing the optimal modular hypothesis for humans (H2), chimpanzees (H1) and gorillas (H9). They were selected as they have the largest negative Z_{CR} values (Table 4). Hypotheses are described in Table 3.

To further explore the previous finding indicating possible variation in the modularity structure across taxa (Fig. 2), a pairwise modularity score (\hat{Z}_{12}) was calculated for every pair of carpals within each genus (Fig. 4). In humans, the modular signals between capitate and lunate, and between trapezium and scaphoid, was significantly lower ($p < 0.05$) than those of the remaining pairs of carpals (capitate and trapezium, and lunate and trapezium). This might suggest that the lunate and capitate have a degree of morphological integration, as do the trapezium and scaphoid. Additionally, the modular signals between capitate and lunate in one module, and trapezium and scaphoid in another, were statistically similar ($\hat{Z}_{12} = 0.26$, $p = 0.28$) (Fig. 4). These findings are consistent with H2 being the model with the best fit for humans (Fig. 2 and 3). In chimpanzees, no pair of carpals exhibits a greater Z_{CR} than any other, which is also expected given that H1 is the optimal modular hypothesis for this genus. As for gorillas, the

capitate and trapezium show a significantly higher modular signal than the lunate and scaphoid ($\hat{Z}_{12}=2.14$, $p=0.03$), which is consistent with the capitate belonging to a different module than the trapezium, as indicated by the hypothesis with the most negative Z_{CR} value (H9). Similarly, the only other significantly different modular signal in gorillas was between the capitate and trapezium, which is higher than that found for the capitate and lunate ($\hat{Z}_{12}=1.90$, $p=0.05$). Both results for gorillas are consistent with H9 being the best model for this genus. However, these results for gorillas do not exclude other hypotheses from being the best modular hypothesis (H1, H8, H10, H12, and H13, Table S5).

Table 4 Covariance ratio (CR) and effect sizes (Z_{CR}) for the modularity hypotheses in the hominid wrist. All CR are statistically significant at $p<0.01$. The Z_{CR} values are depicted in Figure 2 and the pairwise differences in ZCR (\hat{Z}_{12}) are in Tables S3-6. Hypotheses are described in Table 3.

Hypothesis	All		Human		Chimpanzees		Gorillas	
	CR	Z_{CR}	CR	Z_{CR}	CR	Z_{CR}	CR	Z_{CR}
H1	0.64	-8.9	0.55	-8.6	0.57	-8.5	0.53	-8.3
H2	0.75	-7.4	0.56	-9.1	0.7	-6.9	0.63	-7.3
H3	0.81	-5.8	0.76	-5.4	0.76	-5.6	0.63	-7.2
H4	0.80	-5.9	0.74	-5.9	0.66	-7.4	0.64	-7.2
H5	0.75	-5.2	0.61	-6.3	0.67	-5.8	0.66	-5.3
H6	0.60	-8.1	0.62	-6.2	0.71	-5.2	0.76	-3.9
H7	0.77	-4.9	0.7	-5.1	0.71	-5.2	0.48	-7.7
H8	0.81	-4.5	0.66	-5.7	0.65	-6.1	0.56	-6.7
H9	0.81	-6.6	0.57	-7.7	0.6	-7.6	0.48	-8.6
H10	0.73	-7.9	0.59	-7.6	0.63	-7.3	0.61	-6.7
H11	0.65	-8.4	0.6	-7.1	0.61	-7.3	0.57	-7.3
H12	0.63	-6.2	0.59	-7.6	0.6	-7.4	0.56	-7.4
H13	0.74	-6.5	0.6	-7.1	0.61	-7.5	0.51	-8.1
H14	0.63	-8.4	0.58	-7.8	0.63	-7.2	0.66	-6
H15	0	0	0	0	0	0	0	0

Discussion

In this study we aimed to describe the modular pattern in the wrist of hominids and determine whether the pattern and strength of covariation across carpals is shared in humans, chimpanzees, and gorillas. To do this, we used the covariance ratio (CR) (Adams, 2016; Adams and Collyer, 2019) to test the degree to which changes in the capitate, lunate, scaphoid, and trapezium are associated with changes in each of the other bones. Our results indicate that the best fit for the covariation patterns in the wrist of hominids is the hypothesis that indicates that each carpal is its own modular unit (H1), as the level of

covariation between carpals was always smaller than the covariation within carpals (CR in Table 4). This supports previous evidence demonstrating great variability in the shape of carpals across primates (Lewis, 1972; Corruccini, 1978; Kivell et al., 2013). It also indicates that although the hands of humans have become less integrated with the feet in comparison to species with functionally similar use of both structures (Rolian, 2009), it may not mean that the strength of reciprocal relationships across carpals is lower than in apes (H1 in Fig. 2).

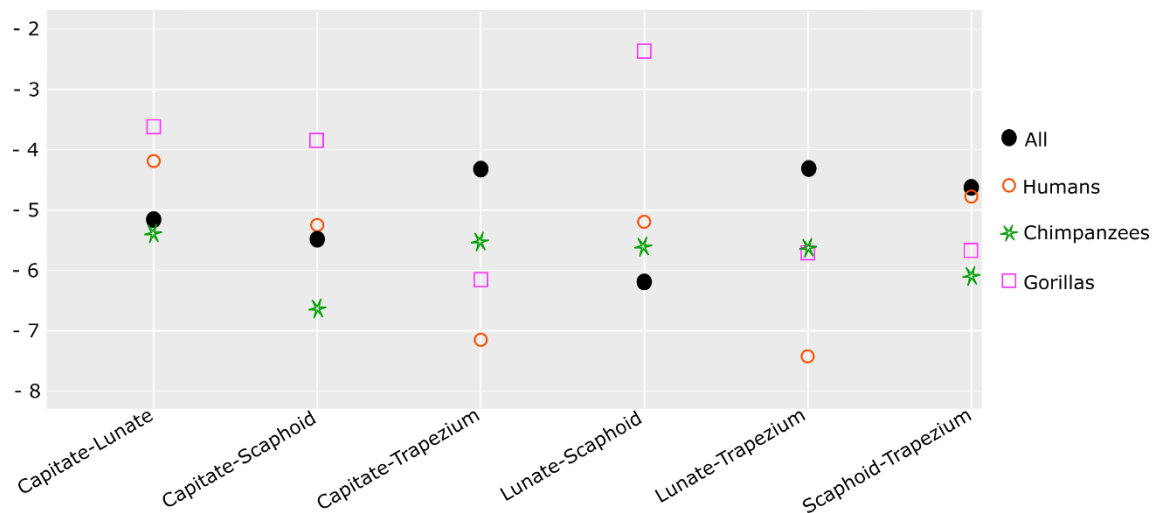


Figure 4 Effect sizes (Z_{CR}) for the optimal modular hypothesis for the wrist in hominids (H1), and for each genus separately.

However, the high level of autonomy of these four carpals indicated by our results requires some caution. First, the generalized Procrustes superimposition procedure, in which each bone was subject to a separate GPA, reduces the possible inflation of the covariance pattern between bones, as compared to the approach that uses one common superimposition and then splits the dataset to assess modularity hypotheses (Cardini, 2019). However, the applied approach (i.e., separate superimpositions) may overestimate modularity, as it discards information related to the relative size and position of the modules (Cardini, 2019). Second, it is also probable that the different covariation structure in the wrist found in some of our analyses for humans, chimpanzees, and gorillas (Fig. 2 and 3, Table 4), favors the simplest of all available hypotheses (H1), particularly when the entire sample is pooled (in terms that suggest no covariation between any of the carpals). In relation to the latter, although H1 was selected as the best model explaining the covariation structure of hominids, the different behavior of the genera when analyzed separately (Fig. 2) and the Z_{CR} comparison between carpal pairs indicate otherwise: that the level of association between some of them vary across taxa. This is true for the levels of covariation between the capitate and lunate, and the trapezium and scaphoid, which are higher for humans when compared to other pairs of carpals (Fig. 4), while for chimpanzees carpal pairs do not present different strengths of covariation. This makes H1 the optimal modular hypothesis for chimpanzees (in which

each carpal corresponds to its own modular unit), while in the case of humans H2 is a better fit (i.e., the capitate and lunate belong to the same modular unit, and the trapezium to another) (Fig. 2 and 3). Gorillas share with humans that the capitate and lunate exhibit a degree of covariation and that the capitate and trapezium belong to different modules (as indicated by H9). However, results were less conclusive for this genus than for the others, as H9 presented the lowest Z_{CR} ; however, these results could not be confirmed when a pairwise modularity score (\hat{Z}_{12}) was calculated for every pair of carpals (Table S5).

According to our analysis, what separates humans from African apes is a stronger degree of covariation between the trapezium and the scaphoid. It is interesting that the radial side of the wrist separates these two groups, as a large proportion of studies dealing with manual differences between apes and humans have focused on the thumb, including the trapeziometacarpal joint, and point to enhanced manipulative capabilities in the former (Hamrick et al., 1998; Marzke et al., 1999, 2010; Tocheri et al., 2008; Feix et al., 2015; Key and Dunmore, 2015). Also, the radio-carpal joint (which involves the scaphoid) has been related to mechanical advantages in accuracy and force generation for the use of tools in humans (Williams et al., 2010, 2014). Further analyses should estimate whether the associated changes of these bones are functionally linked to fine manipulation of objects in humans relative to African apes (Tocheri et al., 2005, 2008; Marzke et al., 2010; Feix et al., 2015). This would require a more detailed landmark configuration and a different statistical approach than the one presented here, as CR cannot be used to describe specific associated shape changes, as principal component analysis and/or partial least squares analysis might (although see Cardini, 2019).

The presence of different modular strengths in the wrist bones of gorillas and chimpanzees (higher modular strength in the latter) is also noteworthy, as the presence of a knuckle-walking complex, common to chimpanzees and gorillas, has long been discussed (Corruccini, 1978; Begun, 1992; Richmond and Strait, 2000; Kivell and Schmitt, 2009; Williams, 2010; Püschel et al., 2020). For instance, Richmond and Strait (2000) proposed that African apes have a unique suite of skeletal traits involving the radiocarpal joint, which is adapted to stabilize the wrist during knuckle-walking, yet others argue that this type of locomotion is not the same biomechanical phenomenon in chimpanzees and gorillas (Inouye, 1994; Kivell and Schmitt, 2009). Our analysis does not indicate that there is a common covariation pattern for chimpanzees and gorillas, different from that of humans, that could allow us to define a potential knuckle-walking complex. This is in line with Williams' (2010) conclusion that there is not a unique pattern of integration between the capitate and third metacarpal that distinguishes knuckle-walkers from non-knuckle-walking taxa.

Conclusions.

Hominids have in common that each carpal covaries mainly with itself (scaphoid, lunate, trapezium and capitate) and with other carpals to a lesser extent. However, there are differences in the covariation strength that they exhibit with other wrist bones. In humans, the trapezium and scaphoid present a significantly lower modular signal with one another than with the remaining bones, and this also occurs with the capitate and lunate. This suggests that there may be associated shape changes between the scaphoid and trapezium, and between the capitate and lunate in humans. In gorillas there are also significant differences in the covariation structure across carpals, which indicates that the capitate and trapezium vary more independently than other pairs of carpals, and that the capitate and lunate covary as they do in humans. Of the three genera, chimpanzees presented the lowest interaction among carpals.

ORCID

Ana Bucchi <https://orcid.org/0000-0002-1247-230X>

Thomas A. Püschel <https://orcid.org/0000-0002-2231-2297>

Antonio Profico <https://orcid.org/0000-0003-2884-7118>

Carlos Lorenzo <https://orcid.org/0000-0001-5706-293X>

Acknowledgements

We are thankful to Alessio Veneziano for his advice on using R. The illustration depicted in Figure 3 was made by the palaeoartist Lou-Octavia Mørch, we really appreciate her help. We are also grateful to the following curators and institutions for the access to the ape specimens: Emmanuel Gilissen (AfricaMuseum), Anneke H. van Heteren and Michael Hiermeier (Zoologische Staatssammlung München), Javier Quesada (Museu de Ciències Naturals de Barcelona), José Miguel Carretero (Universidad de Burgos), and Sergio Almécija (American Museum of Natural History). AB was partially funded by a Becas Chile scholarship, whilst TP was funded by the Leverhulme Trust Early Career Fellowship, ECF-2018-264. This study was funded by research projects AGAUR 2017 SGR 1040 and MICINN-FEDER PGC2018-093925-B-C32.

References

- Adams, D.C., 2016. Evaluating modularity in morphometric data: Challenges with the RV coefficient and a new test measure. *Methods in Ecology and Evolution*. 7, 565–572.
- Adams, D.C., Collyer, M.L., 2019., Comparing the strength of modular signal, and evaluating alternative modular hypotheses, using covariance ratio effect sizes with morphometric data. *Evolution*. 73, 2352-2367.
- Adams, D.C., Collyer, M.L., Kaliontzopoulou, A., 2019. Geomorph: Software for geometric morphometric analysis. R package version 3.0. 6.
- Begun, D.R., 1992. Miocene fossil hominids and the chimp-human clade. *Science*. 257, 1929–1933.
- Bucchi, A., Luengo, J., Fuentes, R., Arellano-Villalón, M., Lorenzo, C., 2020. Recommendations for improving photo quality in close range photogrammetry, exemplified in hand bones of chimpanzees and gorillas. *International Journal of Morphology*. 38, 348–355.
- Cardini, A., 2019. Integration and modularity in Procrustes shape data: is there a risk of spurious results? *Evolutionary Biology*. 46, 90–105.
- CARTA Subject IDs: 3991, 4001, 4003, 4007, 4010, 4073, 4076, 4182. Courtesy of the Center for Academic Research and Training in Anthropogeny/Museum of Primatology at UC San Diego. Retrieved February 11, 2020 from <http://carta.anthropogeny.org>.
- Casillas García, J.A., Adán Álvarez, G.E., 2005. Rescatando la memoria: La actuación arqueológica en el Solar de Caballería y el Convento de San Pablo de Burgos. Instituto Municipal de Cultura del Ayuntamiento de Burgos, Burgos.
- Cignoni, P., Callieri, M., Corsini, M., Dellepiane, M., Ganovelli, F., Ranzuglia, G., (2008, July). Meshlab: an open-source mesh processing tool. In Eurographics Italian chapter conference (pp. 129-136).
- Corruccini, R.S., 1978. Comparative osteometrics of the hominoid wrist joint, with special reference to knuckle-walking. *Journal of Human Evolution*. 7, 307–321.
- Esteve-Altava, B., 2017. In search of morphological modules: a systematic review. *Biological Reviews*. 92, 1332–1347.
- Feix, T., Kivell, T.L., Pouydebat, E., Dollar, A.M., 2015. Estimating thumb-index finger precision grip and manipulation potential in extant and fossil primates. *Journal of the Royal Society Interface*. 12, 20150176.

- Giacomini, G., Scaravelli, D., Herrel, A., Veneziano, A., Russo, D., Brown, R.P., Meloro, C., 2019. 3D photogrammetry of bat skulls: Perspectives for macro-evolutionary analyses. *Evolutionary Biology*. 46, 249-259.
- Hamrick, M.W., Churchill, S.E., Schmitt, D., Hylander, W.L., 1998. EMG of the human flexor pollicis longus muscle: Implications for the evolution of hominid tool use. *Journal of Human Evolution*. 34, 123–136.
- Inouye, S.E., 1994. Ontogeny of knuckle-walking hand postures in African apes. *Journal of Human Evolution*. 26, 459-485.
- Key, A.J.M., Dunmore, C.J., 2015. The evolution of the hominin thumb and the influence exerted by the non-dominant hand during stone tool production. *Journal of Human Evolution*. 78, 60–69.
- Kivell, T.L., 2011. A comparative analysis of the hominin triquetrum (SKX 3498) from Swartkrans, South Africa. *South African Journal of Science*. 107, 60-69.
- Kivell, T., Lemelin, P., Richmond, B.G., Schmitt, D., 2016. *The evolution of the primate hand*. Springer, New York.
- Kivell, T.L., Barros, A.P., Smaers, J.B., 2013. Different evolutionary pathways underlie the morphology of wrist bones in hominoids. *BMC Evolutionary Biology*. 13, 229.
- Kivell, T.L., Schmitt, D., 2009. Independent evolution of knuckle-walking in African apes shows that humans did not evolve from a knuckle-walking ancestor. *Proceedings of the National Academy of Sciences*. 106, 14241–14246.
- Klingenberg, C.P. 2008. Morphological integration and developmental modularity. *Annual Review of Ecology, Evolution, and Systematics*. 39, 115-132.
- Klingenberg, C.P., Marugán-Lobón, J., 2013. Evolutionary covariation in geometric morphometric data: Analyzing integration, modularity, and allometry in a phylogenetic context. *Systematic Biology*. 62, 591–610.
- Lewis, O.J., 1972. Osteological features characterizing the wrists of monkeys and apes, with a reconsideration of this region in *Dryopithecus (Proconsul) africanus*. *American Journal of Physical Anthropology*. 36, 45–58.
- Marzke, M.W., 1983. Joint functions and grips of the *Australopithecus afarensis* hand, with special reference to the region of the capitate. *Journal of Human Evolution*. 12, 197–211.
- Marzke, M.W., 1997. Precision grips, hand morphology, and tools. *American Journal of Physical*

- Anthropology. 102, 91–110.
- Marzke, M.W., Marzke, R.F., Linscheid, R.L., Smutz, P., Steinberg, B., Reece, S., An, K.N., 1999. Chimpanzee thumb muscle cross sections, moment arms and potential torques, and comparisons with humans. *American Journal of Physical Anthropology*. 110, 163–178.
- Marzke, M.W., Tocheri, M.W., Steinberg, B., Femiani, J.D., Reece, S.P., Linscheid, R.L., Orr, C.M., Marzke, R.F., 2010. Comparative 3D quantitative analyses of trapeziometacarpal joint surface curvatures among living catarrhines and fossil hominins. *American Journal of Physical Anthropology*. 141, 38–51.
- Niewoehner, W.A., Weaver, A.H., Trinkaus, E., 1997. Neandertal capitate-metacarpal articular morphology. *American Journal of Physical Anthropology*. 103, 219–233.
- Orr, C.M., 2017. Locomotor hand postures, carpal kinematics during wrist extension, and associated morphology in anthropoid primates. *Anatomical Record*. 300, 382–401.
- Peña, A., 2018. Patterns of integration and modularity in the hominoid wrist (MSc thesis). Retrieved from https://scholarspace.library.gwu.edu/concern/gw_etds/ms35t8905
- Profico, A., Schlager, S., Valoriani, V., Buzi, C., Melchionna, M., Veneziano, A., Raia, P., Moggi-Cecchi, J., Manzi, G., 2018. Package ‘Arothron.’ *American Journal of Physical Anthropology*. 166, 979–986.
- Püschel, T.A., Marcé-Nogué, J., Chamberlain, A.T., Yoxall, A., Sellers, W.I., 2020. The biomechanical importance of the scaphoid-centrale fusion during simulated knuckle-walking and its implications for human locomotor evolution. *Scientific Reports*. 10, 3526.
- Reno, P.L., Mccollum, M.A., Cohn, M.J., Meindl, R.S., Hamrick, M., Lovejoy, C.O., 2008. Patterns of correlation and covariation of anthropoid distal forelimb segments correspond to hoxd expression territories. *Journal of Experimental Zoology Part B: Molecular and Developmental Evolution*. 310, 240–258.
- Richmond, B.G., Strait, D.S., 2000. Evidence that humans evolved from a knuckle-walking ancestor. *Nature*. 404, 382–385.
- Rolian, C., 2009. Integration and evolvability in primate hands and feet. *Evolutionary Biology*. 36, 100–117.
- Rolian, C., Lieberman, D.E., Hallgrímsson, B., 2010. The coevolution of human hands and feet. *Evolution*. 64, 1558–1568.

- Skinner, M.M., Stephens, N.B., Tsegai, Z.J., Foote, A.C., Nguyen, N.H., Gross, T., Pahr, D.H., Hublin, J.-J., Kivell, T.L., 2015. Human-like hand use in *Australopithecus africanus*. *Science*. 347, 395–399.
- Tocheri, M.W., Marzke, M.W., Liu, D., Bae, M., Jones, G.P., Williams, R.C., Razdan, A., 2003. Functional capabilities of modern and fossil hominid hands: Three-dimensional analysis of trapezia. *American Journal of Physical Anthropology*. 122, 101–112.
- Tocheri, M.W., Orr, C.M., Jacofsky, M.C., Marzke, M.W., 2008. The evolutionary history of the hominin hand since the last common ancestor of *Pan* and *Homo*. *Journal of Anatomy*. 212, 544–562.
- Tocheri, M.W., Razdan, A., Williams, R.C., Marzke, M.W., 2005. A 3D quantitative comparison of trapezium and trapezoid relative articular and nonarticular surface areas in modern humans and great apes. *Journal of Human Evolution*. 49, 570–586.
- Tuttle, R.H., 1967. Knuckle-walking and the evolution of hominoid hands. *American Journal of Physical Anthropology*. 26, 171–206.
- Williams, E.M., Gordon, A.D., Richmond, B.G., 2010. Upper limb kinematics and the role of the wrist during stone tool production. *American Journal of Physical Anthropology*. 143, 134–145.
- Williams, E.M., Gordon, A.D., Richmond, B.G., 2014. Biomechanical strategies for accuracy and force generation during stone tool production. *Journal of Human Evolution*. 72, 52–63.
- Williams, S.A., 2010. Morphological integration and the evolution of knuckle-walking. *Journal of Human Evolution*. 58, 432–440.
- Young, N.M., Wagner, G.P., Hallgrímsson, B., 2010. Development and the evolvability of human limbs. *Proceedings of the National Academy of Sciences*. 107, 3400–3405.